

Validity of the Perception Neuron inertial motion capture system for upper body motion analysis

Ryan Sers, Steph Forrester, Esther Moss, Stephen Ward, Jianjia Ma, Massimiliano Zecca

Wolfson School of Mechanical, Electrical and Manufacturing Engineering,

Loughborough University & Leicester Cancer Research Centre, United Kingdom

r.sers@lboro.ac.uk, s.forrester@lboro.ac.uk, em321@leicester.ac.uk, s.ward@lboro.ac.uk,

j.ma@lboro.ac.uk, m.zecca@lboro.ac.uk,

ABSTRACT

The commercially available Perception Neuron motion capture (Mo-Cap) system is a cost effective and easy to use option for motion analysis. However, the accuracy of this system in a practical setting is unknown and needs to be evaluated if it is to be considered for applications that require a specific level of measurement precision. Therefore, the validity of the Mo-Cap system for estimating postural angular kinematics of the upper body was assessed. Upper body motion was evaluated through three-dimensional analysis of functional movements performed by the neck, thorax and shoulders. Range of motion (RoM) estimates were compared to Vicon using Bland-Altman analysis. Systematic biases in neutral to peak RoM differences were all $\leq 4.5^\circ$ and random biases $\leq \pm 4.5^\circ$ except for neck extension where the values were larger. The present findings suggest that the Mo-Cap system is a valid method for assessing the majority of upper body ROM to within 5° .

Keywords

Inertial motion capture, IMUs, Perception Neuron, Vicon, Upper body motion analysis, Validation

1. INTRODUCTION

Qualitative or quantitative measurements are necessary for any procedure involving human motion capture (Mo-Cap). Quantitative analysis requires the measurement of biomechanical variables such as postural angles, pressure distribution, moments and forces produced by the human body [1]. Optoelectronic motion capture is currently considered to be the gold standard in the measurement and quantification of human kinematics in clinical medicine [2,3]. Retroreflective markers are attached to the body and are tracked by cameras which acquire the marker positional data. The positional data can then be used to perform biomechanical analysis, in both static and dynamic conditions. The Vicon (Vicon Motion Systems Ltd., Oxford, UK) optoelectronic system has been shown to track markers with high accuracy, e.g. mean absolute marker tracking errors of 0.15 mm during static trials [3] and 0.2 mm (with corresponding angle errors of 0.3°) during dynamic trials [4]. Therefore, optoelectronic systems such as Vicon are a suitable comparison tool to assess whether alternative systems, e.g. IMU based, provide a sufficiently accurate method for motion analysis [5,6].

Despite this, the requirements to set-up and implement an optoelectronic system are extensive and may not be feasible for many academic institutions and small companies due to the high cost and lengthy set-up times. The system requires a bespoke laboratory

33 environment comprising of high-resolution infrared cameras, as well as a highly trained operator. In addition, optoelectronic systems
34 are confined to the volume of space where the equipment is installed [7,8]. In some instances, optoelectronic systems can be
35 temporarily installed in alternative locations, however this process can also be time consuming to implement and may not be feasible
36 for workplace environments.

37 In recent years, the rapid development in the usability and accuracy of inertial measurement units (IMU's) has seen the
38 introduction of such devices as a viable alternative to optoelectronic systems [9–13]. An IMU is a device which consists of an
39 accelerometer, a magnetometer and a gyroscope, all of which can be either one (1-axis), two (2-axis) or three axis (3-axis) sensors.
40 For most designs, 2-axis sensors are sufficient, however a project such as three-dimensional (3D) motion analysis naturally requires
41 3-axis sensors to accurately detect movement in each direction. These devices are low cost, small and lightweight when compared
42 to alternative systems; however, the main advantages of these devices are the ease of use and portability [2] [14]. The development
43 of sensor fusion algorithms makes it possible to combine raw data from multiple individual sensors, enabling the estimation of 3D
44 spherical coordinates and Euler angles in a global reference domain [15]. An IMU can be secured to a body segment, thereby
45 providing kinematic motion data on that anatomical area making it possible to evaluate human movement as well as reducing the
46 aforementioned operational limitations present in other Mo-Cap systems [7]. IMU's have been successfully used to estimate lower
47 limb joint and pelvis angular kinematics [14] [16,17], upper body posture during gait analysis [9] and full body motion analysis [10]
48 [18]. In a review by Lopez-Nava and Munoz-Melendez [1], 75% of the 37 studies comparing IMU's to a reference system used an
49 optoelectronic system as the gold standard evaluation method.

50 The Perception Neuron inertial Mo-Cap system (NOITOM Ltd, China) was primarily developed for gaming and virtual
51 reality applications [19] and, to the authors' knowledge, has yet to be validated for applications that require a higher level of
52 measurement accuracy such as work place posture analysis. Indeed, the published research utilizing this system has not reported a
53 validation of the outputs [20,21]. The current intended use for the system is to track the posture of surgeons in both simulated and
54 real environments, therefore requiring a system of a known precision that is accurate enough to prevent misinterpretation of the
55 clinical postural data. The issue of surgeon musculoskeletal disorders (MSDs) is well-known [22], and most epidemiologic work to
56 better understand and prevent such disorders involves optoelectronic tracking of the surgeon [23]. However, in real environments
57 these systems cannot be used because a direct line of sight cannot be maintained in an operating theatre (OT), together with the
58 portability issues detailed above for optoelectronic systems. The operational constraints of optoelectronic systems for this
59 application highlight the need for a Mo-Cap system which offers portability in the data acquisition while maintaining an acceptable
60 level of measurement accuracy.

61 Therefore, the purpose of this study was to evaluate the joint angle range of motion (ROM) data provided by the Perception
62 Neuron inertial Mo-Cap system (IMU suit) through comparison to a gold standard optoelectronic system (Vicon). The anatomical
63 areas evaluated included three-dimensional angles of the neck and thorax together with shoulder abduction. These areas were
64 evaluated because they are utilized significantly by surgeons during surgery [24]. The methodological design was developed to

65 determine whether the IMU suit was suitable for the assessment of surgeon ergonomics during surgery, the primary future
66 application of the system.

67 2. MATERIALS AND METHODS

68 2.1. Participants

69 Eight healthy individuals (5 male and 3 female) volunteered in the study. The participants age ranged from 20 to 25 years,
70 height from 1.63 m to 1.91 m and body mass from 56.5 kg to 104.0 kg. Each participant provided written consent before taking part
71 in the study which was approved by the Loughborough University ethical committee. Exclusion criterion was physical injury or
72 self-reported musculoskeletal disorders at the time of testing.

74 2.2. Instrumentation

75 The Perception Neuron IMU suit was used. This system provides the ability to perform calibrated full body inertial motion
76 capture in real time, while streaming and logging kinematic data into their proprietary software (Axis Neuron). Within the system's
77 proprietary software, a three-dimensional reconstruction of the suit's wearer is produced and, once calibrated (see 2.2.1), coherent
78 motion of the wearer can be visualized for all body segments. The suit has several operating modes which include single arm, upper
79 body and full body capture. Each mode can utilize a different number of neurons (IMUs) ranging from three in single arm mode, to
80 32 in full body mode however, within this study the system was configured in the full-body 18-neuron mode. This mode was used
81 despite the study being an upper body validation because of its suitability for the intended surgery-based future application, where
82 full-body capture is an option but not essential. Therefore, assessing this mode allows for this future flexibility and ensures a
83 validation has taken place on this operating mode, as measurement discrepancies in differing operating modes is possible. Each
84 neuron (12.5 mm x 13.1 mm x 4.3 mm) is an IMU consisting of a 3-axis gyroscope (± 2000 dps), 3-axis magnetometer and 3-axis
85 accelerometer ($\pm 16g$) [19]. For the purpose of this study only 7 physical neurons were used for analysis (Table 1), as these are the
86 major areas that are utilized considerably by surgeons within the surgery-based application [24]. Neurons were placed in designated
87 sockets on the suit and secured via Velcro strapping on the anatomical landmarks (Figure 1). In addition to the neuron data, the
88 proprietary algorithms for the IMU suit also provided Euler angles for 'virtual' neurons positioned at the neck and approximately
89 the T3, T8, and L1 vertebrae. The IMU suit also comes with a hub, which allows the connection and powering of all neurons in
90 series though wired connections. The hub aggregates individual sensor data and transfers it to a dedicated router wirelessly via
91 TCP/IP. Data is then streamed directly into the suit's propriety software (Axis Neuron version 3.8.42.8308) in real time through a
92 predefined IP and port. The IP address and port number of the wireless router were matched with the proprietary software and hub
93 prior to data acquisition allowing the data to stream into the software.

Table 1 - Perception Neuron IMU positions (Figure 1) [19]

Number	Anatomical position
1	Head
2	Upper spine (C7)
3 & 4	Acromion (L & R)
5 & 6	Centre of humerus (L & R)
7	Lower spine (Just above hips)

96

Table 2 - Upper Body Plug-In-Gait Marker positions (Figure 1) [25]

Number	Anatomical position
1 & 2	Front of Head (L & R)
3 & 4	Back of Head (L & R)
5	Clavicle
6	Sternum
7	Upper spine (C7)
8	Right Back (Latissimus Dorsi)
9	Lower/middle spine (T10)
10 & 11	Shoulder (L & R)
12 & 13	Upper arm (L & R)
14 & 15	Elbow (L & R)
16 & 17	Forearm (L & R)
18 & 19	Wrist (Distal end of the radius) (L & R)
20 & 21	Wrist (Distal end of the ulna) (L & R)
22 & 23	Dorsal side of hand (L & R)

97

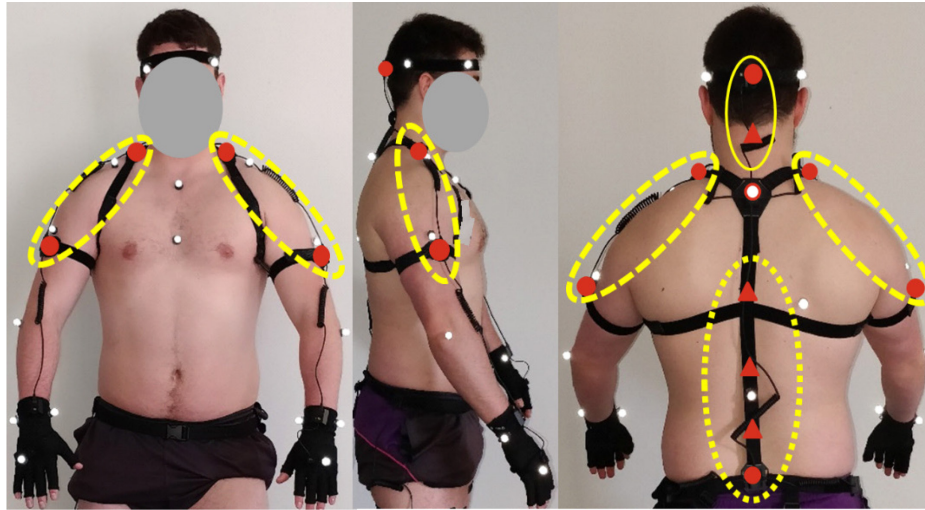


Figure 1 - IMU suit and marker set fitted to a participant (red circles show physical neuron positions and red triangles show virtual neuron positions, head and neck neurons are shown within the solid circle in the right image, the four spinal neurons are also shown in the right image within the dotted circle and the shoulder neurons are shown within the dashed circle in the left image)

98

99

In parallel, a Vicon optoelectronic system consisting of twelve cameras was used as the gold standard reference system. The upper body plug-in gait marker set (Figure 1 and Table 2) was used to capture the data in Nexus 2.6.1 [25]. The IMU suit and marker set were worn at the same time to ensure concurrent data acquisition. Both the IMU and Vicon data were acquired at 120 Hz and synchronized off-line during data processing. Prior to testing the experimental area was cleared of metallic objects to ensure that the magnetometers within the IMU's would not be subject to high magnetic fields, which would adversely affect the accuracy of the motion capture data [25].

105

Many studies comparing IMUs to optoelectronic reference systems place the markers directly on the IMUs and, therefore, solely compare measurement accuracy of the optical and inertial system. However, to obtain an accurate representation of IMU system performance, the retroreflective markers were placed on anatomical landmarks such that the ability of the IMU's to track human motion could be assessed.

109

2.2.1. IMU suit calibration

111

The IMU suit required the input of anthropometric data comprising all upper body segment lengths which were obtained through measurement with a cloth tape measure [19]. The manufacturer recommended calibration process was utilized and comprised of four separate positions: 1) a steady pose where the user was sat down at a desk with their palms face down on the table; 2) a standing T pose where the shoulders were abducted by 90° with the palms facing to the floor; 3) a standing A pose with the shoulders in a neutral posture and palms down at the side of the legs and, 4) an S pose where the knees were flexed by approximately 45° and the shoulders flexed by 90° with the palms facing the floor. Each pose was held for several seconds as per calibration guidelines [19].

118

2.2.2. Optoelectronic system calibration

119

120 The upper body plug-in-gait model in Vicon required body mass and height which were obtained prior to data collection.
121 The Vicon hardware was calibrated following the Vicon Nexus 2 user guide instructions [25]. Firstly, the twelve high-resolution
122 infrared cameras were set-up for the experimental capture volume and the focus of each camera optimized to capture markers of 14
123 mm in diameter in this space. The cameras were masked to prevent unwanted reflections in the capture volume and the calibration
124 wand (L frame) was used for camera calibration. The refinement value was set to 2000 frames and the threshold for a successful
125 calibration was set as image errors < 0.2 for all cameras. The volume origin was then set using the calibration wand.

126 2.3. *Experimental protocol*

127 To evaluate the IMU suit for upper body motion analysis, a functional movement protocol was generated. This
128 encompassed: neck flexion/extension, neck lateral flexion, neck rotation, torso flexion/extension, torso lateral flexion, torso rotation
129 and shoulder abduction. Neck flexion/extension was defined as the motion of the head relative to the torso in the sagittal plane, neck
130 lateral flexion was defined as the motion of the head relative to the torso in the coronal plane and neck rotation was defined as the
131 motion of the head relative to the torso in the transverse plane. Torso flexion/extension was defined relative to the global sagittal
132 plane, torso lateral flexion was defined relative to the global coronal plane. Additionally, shoulder abduction or elevation was defined
133 as movement of the arm away from the body in the global coronal plane (Figure 2).

134 Each movement was performed twice by the participant at self-selected fast and slow speeds. The only guidance given was
135 to ensure that the slow trial was conducted at a slower speed than the fast trial. The use of different movement speeds has been
136 previously implemented as a method to show potential limitations in system performance [26]. Moreover, a complete trial would
137 begin with the participant assuming the anatomical position (Figure 1), then they would execute the functional movement and return
138 to the initial anatomical position. In total, 16 movement trials were performed by each participant ($2 \times$ neck flexion/extension, $2 \times$
139 neck lateral bending, $2 \times$ neck axial rotation, $2 \times$ thorax flexion/extension, $2 \times$ thorax lateral bending, $2 \times$ thorax axial rotation, 2
140 \times shoulder abduction for each shoulder).

142 2.4. *Data analysis*

143 2.4.1. *IMU post-processing*

144 Several post-processing steps were taken to ensure the IMU data was comparable to the Vicon data. This included
145 computing the IMU angles on the same basis as the Vicon plug-in-gait angles. For the neck, the head angles needed to be expressed
146 relative to the thorax (Table 3). To achieve this output from the IMU system, the angles produced by the head and neck neurons
147 (which are computed separately by default, head angles are calculated about the neck and neck angles about the thorax) were
148 combined using quaternion multiplication, to obtain overall angles of the head relative to the thorax. This process was repeated for
149 the thorax and shoulder angular outputs for their respective neurons (Table 3). The thorax data for both systems was absolute (in
150 the global reference frame) and were computed as the angles between the thorax and the laboratory coordinate system. To achieve
151 this output from the IMU suit, the angles produced by the spinal neurons were combined using quaternion multiplication from the
152 T3 down to the root bone (hips) in order to obtain the orientation of the thorax in a global reference frame.

153

154

Table 3 - Angle outputs compared between systems

Joint/Segment	Description	IMU neurons used
Neck	Angles of the head relative to the thorax	Head & Neck
Shoulder	Angles of the upper arm relative to the thorax	Humerus & Acromion
Thorax	Angles of the thorax in the global coordinate system	T3, T8, L1 & Lower spine

155

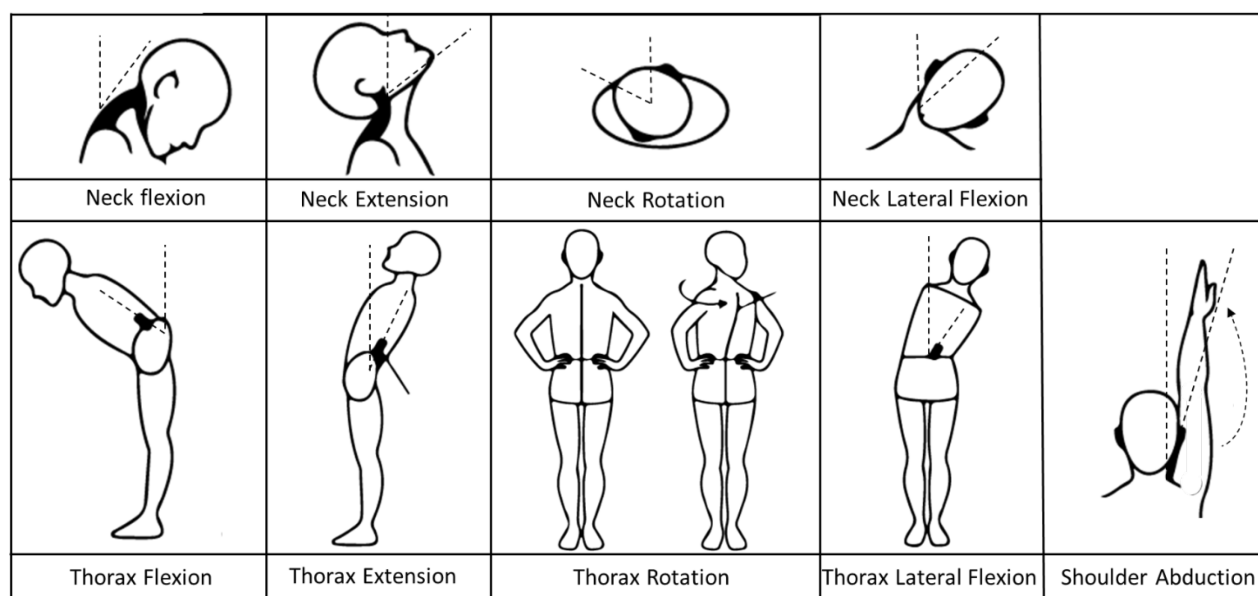


Figure 2 – The functional movements completed within this study

156

157

158

159

160

161

162

163

164

165

166

167

168

The shoulder data produced by Vicon plug-in-gait model is relative to the thorax. Therefore, to acquire a comparable result for the IMU suit, the angles produced by the upper arm and shoulder neurons were combined using quaternion multiplication. This method was preferred to Euler angles with rotation matrices because during certain rotation sequences it was clear that gimbal lock had occurred, degenerating the three degree of freedom attitude description into two, resulting in largely erroneous and distorted data [27]. Quaternions represent a rotation in 3D space and consist of a real component and three imaginary components and can be considered as a 4D vector. Most importantly, quaternions provide an alternative measuring technique that is not subject to singularities such as gimbal lock [27]. Quaternion multiplication is non-commutative, therefore it was crucial to multiply the rotations in the correct order [28].

2.4.2. Vicon post-processing

The marker data was reconstructed and labelled as per the plug-in gait upper body template [25]. Marker trajectories were gap filled using the spline, pattern and rigid body fill depending on the size and location of the gaps. They were then filtered using

169 a fourth order Butterworth low pass filter (6 Hz) to remove any high frequency noise. The dynamic plug-in gait pipeline was then
170 executed, and the angle time series results exported as an ASCII (.csv) file.

172 2.4.3. Additional post-processing steps

173 The angular output from the IMU suit consisted of estimated roll, pitch and yaw angles, which were considered as the
174 anatomical angles for lateral bending, flexion/extension and axial rotation respectively. The upper body plug-in gait model in Vicon
175 computes the angular kinematic data in the YXZ rotation order [25]. With reference to the capture volume, this rotation order
176 corresponds to an initial rotation in the sagittal plane, followed by the coronal plane and then the transverse plane. The rotation order
177 was matched in the IMU system when converting from Quaternions to Euler angles, as the axis definitions for each system are
178 different by default. The IMU data was also filtered using a fourth order Butterworth low pass filter (6 Hz) to remove high frequency
179 noise. The outputs from both systems were then synchronized using a peak detection algorithm and cropped to the same time range
180 in MATLAB (Matlab, MathWorks, Natick, MA, USA) [9] [29].

181 The angle time series from both systems were normalized to the mean of the first twenty data points in each cropped trial.
182 This process eliminated systematic offset present between systems. Since this study was primarily concerned with how well the suit
183 tracks range of motion (ROM) of upper body movements, any offset present can be removed without interfering with this analysis.
184 To evaluate the IMU systems angular outputs, rotation about the primary axis for each of the functional movements were directly
185 compared between systems. To carry out analysis on the IMU data, the CALC file type was broadcast via network protocols
186 (TCP/IP) in a binary format, from Axis Neuron into MATLAB. The equivalent Vicon ASCII file was also imported into MATLAB.

188 2.4. Statistical analysis

189 To compare the postural angular outputs from either system, several metrics were calculated. These consisted of: (i) Bland
190 Altman analysis (BA) on the neutral (starting anatomical angle) to peak (maximum angle for a given functional movement) ROM
191 values to assess for systematic and random biases [31]; (ii) paired t-tests on the mean differences in ROM between systems to test
192 for significance in the systematic bias values;

$$193 \quad t = \frac{\bar{o}}{s / \sqrt{n}} \quad (1)$$

194 where \bar{o} is the mean difference, s is the sample variance and n is the number of participants [32]. Once a t value was determined,
195 the t-test table was then referred to with a significance value of 5%. It should also be noted that the degrees of freedom (df) used
within this test are:

$$196 \quad df = n - 1 \quad (2)$$

(iii) The root mean squared difference (RMSD) between waveforms generated by the two systems as an overall measure of waveform agreement,

$$RMSD = \sqrt{\frac{\sum_{f=1}^F (\hat{p}_f - p_f)^2}{F}} \quad (3)$$

where \hat{p}_f is the “predicted” value from the IMU suit, p_f is the observed value from Vicon, both for the f th time point and within F , the total number of time points [33]. (iv) A waveform similarity assessment Equations ((4)), ((5)) and ((6)) using the coefficient of multiple correlation (CMC) [34]:

$$CMC = \sqrt{1 - \frac{\sum_{m=1}^M \sum_{f=1}^F (\theta_{mf} - \bar{\theta}_f)^2 / F(M - 1)}{\sum_{m=1}^M \sum_{f=1}^F (\theta_{mf} - \bar{\theta})^2 / (MF - 1)}} \quad (4)$$

where θ_{mf} is the angle at time point f that has been measured by the method M . Additionally, $M = 2$ as there are two methods and F is the total number of time points. $\bar{\theta}_f$ is the mean angle at time point f between the angles measured by the two systems:

$$\bar{\theta}_f = \frac{1}{m} \sum_{m=1}^M \theta_{mf} \quad (5)$$

$\bar{\theta}$ is the grand mean for the movement trial among these two methods:

$$\bar{\theta} = \sum_{m=1}^M \sum_{f=1}^F \theta_{mf} \quad (6)$$

CMC values have been used previously to quantify waveform agreement [16]. Excellent agreement was defined as being between 0.95 - 1, very good between 0.85 - 0.94 and good between 0.75 - 0.84. The CMC measures the overall similarity of waveforms, considering the concurrent effects of differences in correlation and gain [34]. All statistical analyses were performed in MATLAB.

3. RESULTS

Postural kinematics from 128 functional movement trials (8 participants \times 8 movements \times 2 speeds) were analyzed. Exemplar ROM angle waveforms for both systems and all anatomical areas are displayed in Figure 3. Flexion and extension movements have been considered separately for the agreement analysis since the ROM magnitudes differed between the two directions due to the significant anatomical difference in the movements. Lateral bending to the left and right and axial rotation to the left and right have not been separated since they are symmetrical movements repeated to either side with similar ROM magnitudes.

218 3.1 RoM Limits of Agreement analysis

219 The mean neutral to peak RoM differences (systematic bias) were all below 4.5°, except for neck extension (6.1°) (Figure 4
 220 and Table 4). For all angles the IMU suit systematically under-estimated RoM. In general, slow trials resulted in larger mean RoM
 221 differences than fast trials; however, this difference was small. The limits of agreement (random bias) were, in the majority of cases,
 222 slightly larger although the majority did not exceed ±4.5°, except again neck extension (±9.0°) without any obvious speed of
 223 movement effects. Paired t-tests revealed that all the mean RoM differences were significantly different from zero (p<0.05).

224 3.2 Waveform analysis

225 The root mean squared differences between system waveforms indicated very good agreement with all below 4° and all
 226 except neck flexion/extension and shoulder abduction below 2.5° (Table 4). There was no obvious effect of speed of movement on
 227 these values. Similarly, mean CMC values for all 14 waveforms were 0.99, reinforcing the excellent overall waveform agreement.
 228

Table 4 – Mean neutral to peak angle RoM differences (SD) and waveform RMSDs (SD) between the IMU and Vicon systems. Left and right shoulder data have been combined.

	Neck						Thorax						Shoulders	
	Flexion/Extension		Lateral bend		Axial rotation		Flexion/Extension		Lateral Bend		Axial Rotation		Abduction	
	Slow	Fast	Slow	Fast	Slow	Fast	Slow	Fast	Slow	Fast	Slow	Fast	Slow	Fast
Mean neutral to peak RoM difference (°)	F: 4.2 (2.5) E: 6.8 (4.7)	F: 4.3 (2.3) E: 5.4 (4.7)	2.9 (2.1)	3.6 (2.9)	3.0 (2.4)	1.7 (1.6)	F: 3.4 (3.1) E: 2.4 (2.1)	F: 2.5 (1.3) E: 1.4 (1.1)	1.8 (1.4)	1.7 (1.9)	3.0 (2.0)	2.7 (1.8)	3.6 (1.7)	3.1 (2.4)
Mean RMSD (°)	3.7 (1.2)	2.7 (0.6)	2.0 (1.1)	2.3 (1.2)	2.5 (1.2)	1.9 (0.8)	2.3 (1.5)	1.6 (0.6)	1.3 (0.7)	1.4 (0.9)	2.2 (0.7)	2.4 (0.7)	3.2 (1.1)	2.9 (1.5)

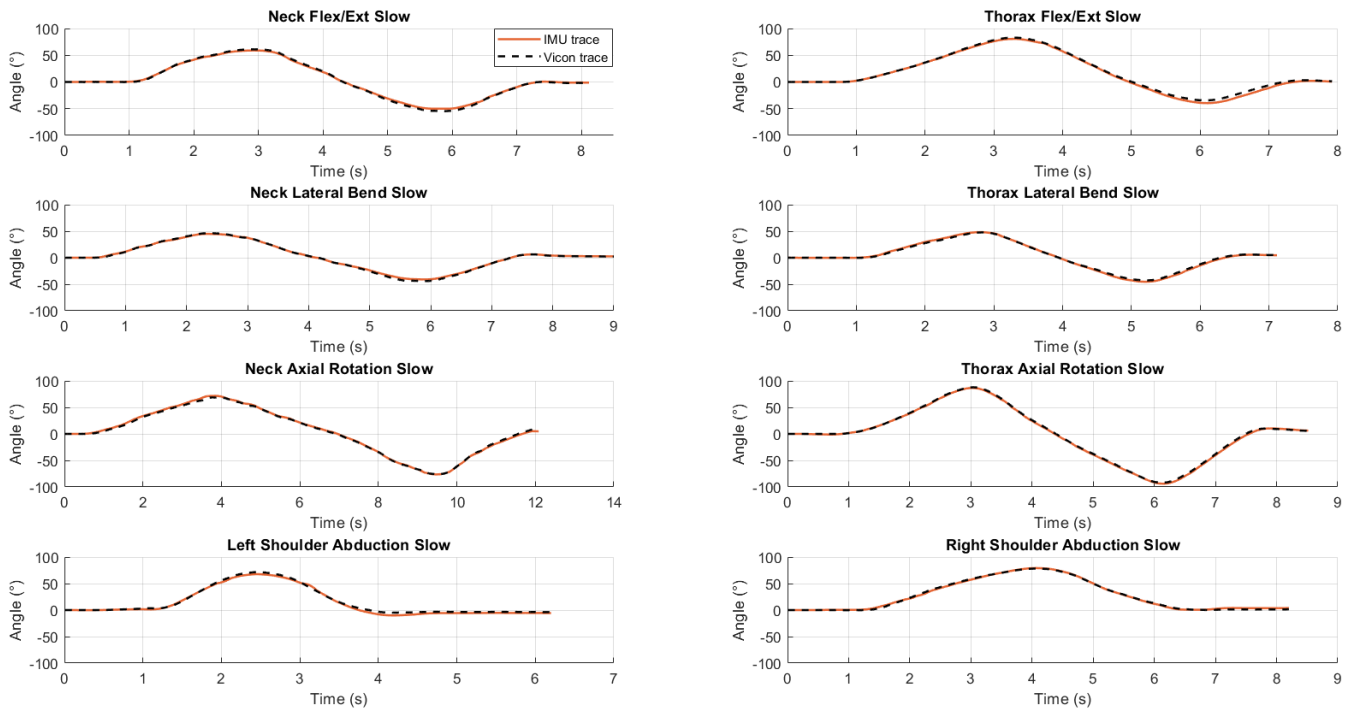


Figure 3 - Exemplar postural angles for slow functional movement trials. Vicon (dotted black line) and the IMU suit (solid green line) during representative movement trials for the neck, thorax and shoulders. The data shown are for one participant.

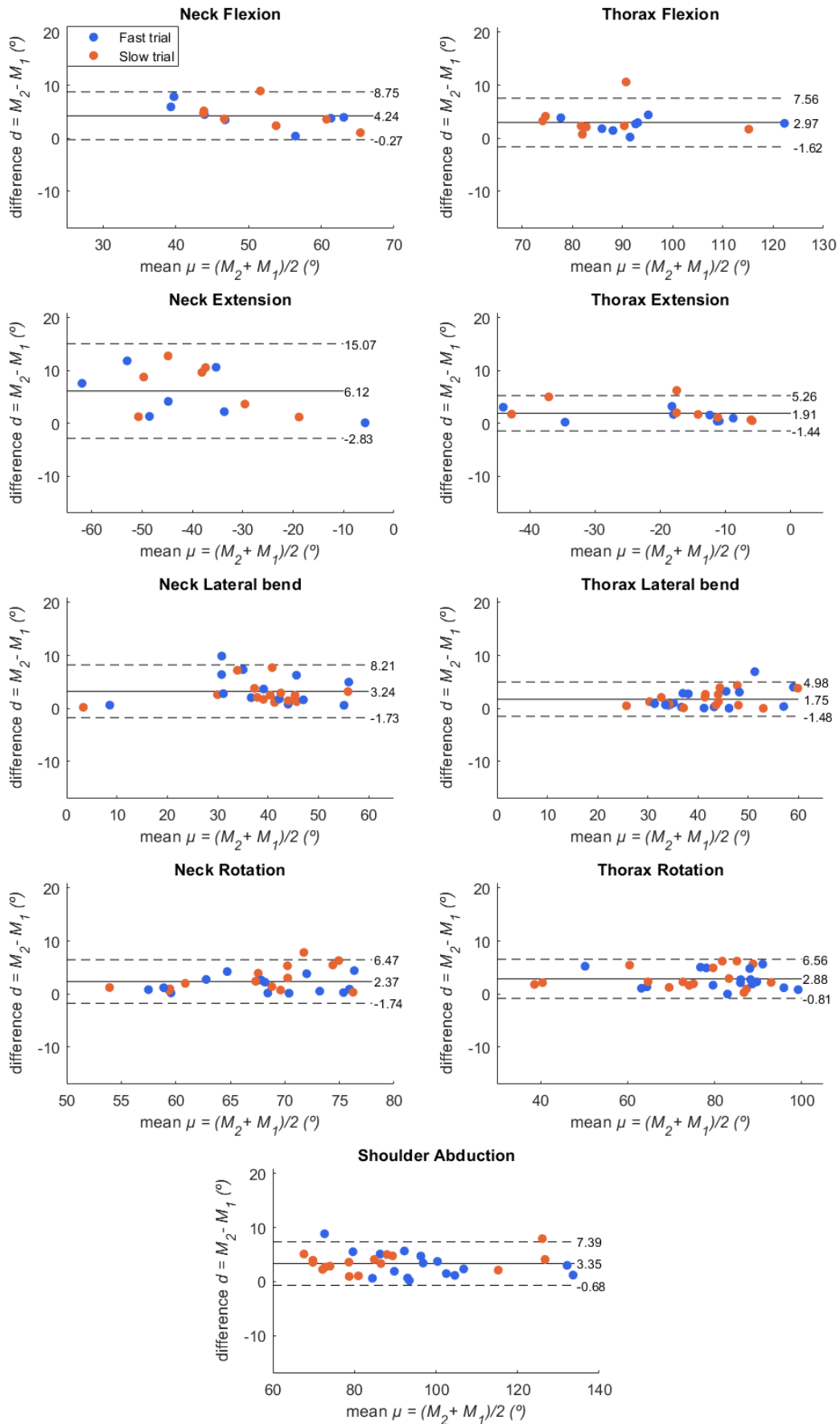


Figure 4 - Bland-Altman plots for each absolute angle. M_2 is Vicon and M_1 is the IMU suit. The solid horizontal line represents the mean difference and the dashed horizontal lines represent the upper and lower 95% confidence intervals (limits of agreement).

4. DISCUSSION

The aim of this study was to validate the Perception Neuron IMU suit in its ability to measure postural angular kinematics of the upper body. To do this, 128 functional movement trials were performed, and the RoM results were compared to a gold standard in optoelectronic motion capture (Vicon). Statistical analyses comprised of Bland-Altman analysis to assess for systematic and random biases in the neutral to peak angle differences and RMSD and CMC for comparison of overall waveforms.

Bland-Altman analysis revealed that the systematic and random biases for the majority of angle RoM differences were $\leq 4.5^\circ$ with the exception of neck extension where the values were larger at 6.1° and $\pm 9.0^\circ$ respectively. The IMU suit systematically underestimated the neutral to peak RoM. A small systematic bias was expected since the Vicon markers and IMU suit inertial sensors were positioned independently on the body [35–38]. As this bias can be accounted for in the interpretation of the data, it does not represent a major limitation in the use of the suit for applications where a specific level of accuracy is needed. Random bias is, arguably, more important from a consideration of future applications and the results of this study suggest that generally the RoM precision is in the range 3° – 5° for all angles considered except neck extension where the value is much larger at 9° . This suggests that the suit may be suitable for applications where it is good enough to detect RoMs to the nearest 3° – 5° (except neck extension). Following the research by McGinley et al. [39] and Cuesta-Vargas et al. [40] it is suggested that for most common clinical applications an error of $\leq 2^\circ$ is considered acceptable, as these errors are in most cases too small to require interpretation. Measurement errors of between 2° and 5° are also likely to be regarded as satisfactory but may require consideration when interpreting the data. While measurement errors of more than 5° should raise concern and may be large enough to mislead the clinical interpretation of the data [39]. On this basis, the IMU suit demonstrates satisfactory measurement errors for all tested angles except neck extension for which the suit data should be treated with caution.

The waveform measures of RMSDs and CMC gave excellent overall agreement between measurement systems (all RMSDs $< 4^\circ$ and average CMC of 0.99), indicating the IMU suit and Vicon reference system produced highly similar waveform characteristics. Both the RoM difference and RMSD results obtained in this study are in agreement with, or in many cases better than, results found in similar studies comparing IMU based measurement systems with optoelectronic Mo-Cap systems [7,8] [14] [35] [41]. Bolink et al. [14] compared IMU's to an optoelectronic system to validate the IMU's capability to assess pelvic orientation angles during gait, sit and stand transfers and step-up transfers, yielding RMSD results of between 2.7° and 4.4° for the frontal plane and between 4.4° and 8.9° for the sagittal plane. Kang and Gross [9] compared the same systems with the objective of validating IMU's for the use in estimating upper body posture, RMSDs reported from this study were 2.9° , 2.7° and 2.2° for head flexion, thorax flexion and shoulder shrug elevation respectively. Lebel et al. [7] compared commercially available IMU's to Mo-Cap by attaching the IMU's and reflective markers onto an artificial object moving under laboratory conditions and reported RoM differences of 3.1° in slow motion conditions ($90^\circ/\text{s}$) and statistically significant greater differences of 7.1° in fast motion conditions ($180^\circ/\text{s}$). Takeda et al. [41] compared hip and knee joint motion during gait evaluated simultaneously by IMU and Mo-Cap systems, with the retroreflective markers attached to anatomical landmarks and reported mean RMSDs of 8.7° for hip flexion/extension, 6.7° for knee joint flexion/extension and a mean RMSD of 4.9° for hip abduction/adduction. Finally, Seel et al. [35] compared IMU and

265 Mo-Cap systems when measuring knee and ankle flexion/extension during gait of a trans-femoral amputee between the prosthesis
266 and the soft tissue leg, reporting RMSDs of 0.7° to 0.8° for the prosthesis leg and 1.6° to 3.3° for the soft tissue leg. This final study
267 highlights the effect of soft tissue motion on the measurements in accentuating the difference between systems.

268 Some of the observed differences between systems in this study will have been a result of the retroreflective marker
269 placement. The markers were placed on soft tissue anatomical landmarks rather than attached to the IMU's; the latter has been the
270 preferred method in many IMU validation studies to minimize error [9,10] [35]. Markers were placed on anatomical landmarks so
271 that motion analysis could be analysed rather than absolute accuracy of the sensors. As expected, previous studies that placed
272 retroreflective markers on anatomical landmarks obtained significantly larger RMSDs than studies that placed the markers on the
273 IMU's [35]. Furthermore, and in agreement with the results obtained here, studies that placed the markers on landmarks rather than
274 directly on the sensors have also reported a systematic underestimation in angular ROM measurement for the IMU system compared
275 to Vicon [42]. This may be the result of the markers being positioned on the extremities of segments, with the consequent potential
276 to undergo slightly larger angular displacements, compared to the IMU sensors which are positioned more centrally on the segments.

277 As discussed above, the IMU angle outputs generally demonstrated good agreement with those from Vicon, with relatively
278 small neutral to peak angle RoM differences. However, it was clear that the IMU suit struggled to provide acceptable measurements
279 for neck extension RoM. Neck extension angle was calculated from the head neuron and the virtual neck neuron, with little
280 information provided by Perception Neuron on how data for the latter was obtained. This heavy reliance on a virtual neuron,
281 particularly around the upper spine where flexion/extension is a complex motion, appears the most likely reasoning for the issue
282 with the neck extension angles. More generally, it is expected that caution is needed in data from the IMU suit which is heavily
283 reliant on a virtual neuron. In contrast, shoulder angle relied only on real neurons and whilst the thorax involved a mix of real and
284 virtual neurons as a segment angle expressed in the global reference frame it would not have suffered to the same extent as the neck.
285 Some limitations of this study should be acknowledged when interpreting the results. The two systems were compared based on
286 eight able-bodied participants all of a very similar age (20–25 yrs.). This relatively small sample size may have limited the outputs
287 from the Bland-Altman analysis where a larger sample size would provide better estimations of the systematic and random biases.
288 Moreover, a small sample size may limit the generalizability of the relationship between the two systems by not adequately
289 representing the broader population, e.g. in soft tissue, body structure and pathological movement characteristics all of which have
290 the potential to influence the relationship between the systems [37,38]. Despite these limitations, the sample size chosen reflects
291 that used in similar IMU validation studies [9] [16,17] [29] [33]. None of the functional movements included within the protocol
292 were constrained and only the primary axis of each movement was analysed, i.e. IMU suit performance about the lesser axes was
293 not considered. This methodology was implemented since the focus was on evaluating the IMU suit when worn by human
294 participants performing natural movements relevant to the intended future application. Finally, trial duration was less than 10
295 seconds, meaning that the long-term usability and reliability of the IMU suit was not evaluated. In particular, the long-term effects
296 of gyroscopic drift or magnetic interference have not been assessed. Therefore, future analysis should include trials of longer
297 duration, i.e. from several minutes to several hours, in both static and dynamic conditions to identify any limitations in the

software's proprietary algorithm or sensors with respect to long capture times which would impact the quality and validity of the kinematic data. Moreover, a lower body assessment should be completed against the gold standard to determine the feasibility of a comprehensive full body kinematic analysis. The intended application requires an upper or full body assessment of surgeon postural motion during simulated laparoscopic surgery; this can last for multiple hours; therefore, the suit must be shown to acquire data reliably for extended durations.

5. CONCLUSION

The validity of a commercially available Perception Neuron IMU suit was examined in terms of its ability to measure upper body postural angle RoM during a range of functional movements. In most cases the IMU suit performed adequately with systematic and random biases in mean neutral to peak RoM differences of $\leq 5^\circ$ and mean waveform RMSDs of $< 4^\circ$ indicating a relatively high level of concurrency throughout each movement. The main exception was neck extension where the level of agreement was substantially poorer indicating the need for extreme caution when interpreting IMU suit data for this angle. Movement speed appeared to have a negligible effect on the performance of the IMU suit. Thus, the IMU suit appears a valid method for assessing upper body motion where a measurement precision of 3° – 5° is sufficient. This level of measurement precision is adequate for the intended application of objectively quantifying surgeon posture. When referring to the previously discussed acceptable error margins and the accuracy of similar measurement systems, the margin of error found for almost all functional movements within this study is sufficient to not cause gross misinterpretation of optimal and sub-optimal postures. It should be noted that the integrity of these conclusions is based on careful calibration and set up of the IMU suit to ensure correct positioning and minimal superficial movement of the sensors.

ACKNOWLEDGEMENTS

This work has been partially supported by the LU-HEFCE catalyst grant and by the LU-EESE startup grant. The authors would like to thank all participants, Josh Turner and Ben Clark for their assistance and time with the data collection.

CONFLICTS OF INTEREST

The authors have no association with NOITOM Ltd, the developers of the inertial Mo-Cap system or with Vicon Motion systems.

REFERENCES

- [1] I.H. Lopez-Nava, A. Munoz-Melendez, Wearable Inertial Sensors for Human Motion Analysis: A Review, *IEEE Sens. J.* 16 (2016) 7821–7834. doi:10.1109/JSEN.2016.2609392.
- [2] W.Y. Wong, M.S. Wong, K.H. Lo, Clinical applications of sensors for human posture and movement analysis: A review, *Prosthet. Orthot. Int.* 31 (2007) 62–75. doi:10.1080/03093640600983949.
- [3] P. Merriaux, Y. Dupuis, R. Boutteau, P. Vasseur, X. Savatier, A study of vicon system positioning performance, *Sensors (Switzerland)*. 17 (2017) 1–18. doi:10.3390/s17071591.

- 329 [4] A.C. Smith, Coach informed biomechanical analysis of the golf swing, Loughborough University, 2013.
330 <https://dspace.lboro.ac.uk/2134/13594>.
- 331 [5] P. Eichelberger, M. Ferraro, U. Minder, T. Denton, A. Blasimann, F. Krause, H. Baur, Analysis of accuracy in optical
332 motion capture – A protocol for laboratory setup evaluation, *J. Biomech.* 49 (2016) 2085–2088.
333 doi:10.1016/j.jbiomech.2016.05.007.
- 334 [6] S. Sessa, M. Zecca, Z. Lin, L. Bartolomeo, H. Ishii, A. Takanishi, A Methodology for the Performance Evaluation of
335 Inertial Measurement Units, *J. Intell. Robot. Syst.* 71 (2013) 143–157. doi:10.1007/s10846-012-9772-8.
- 336 [7] K. Lebel, P. Boissy, M. Hamel, C. Duval, Inertial measures of motion for clinical biomechanics: Comparative assessment
337 of accuracy under controlled conditions - Effect of velocity, *PLoS One.* 8 (2013). doi:10.1371/journal.pone.0079945.
- 338 [8] J.C. Van Den Noort, A. Ferrari, A.G. Cutti, J.G. Becher, J. Harlaar, Gait analysis in children with cerebral palsy via
339 inertial and magnetic sensors, *Med. Biol. Eng. Comput.* 51 (2013) 377–386. doi:10.1007/s11517-012-1006-5.
- 340 [9] G.E. Kang, M.M. Gross, Concurrent validation of magnetic and inertial measurement units in estimating upper body
341 posture during gait, *Meas. J. Int. Meas. Confed.* 82 (2016) 240–245. doi:10.1016/j.measurement.2016.01.007.
- 342 [10] X. Robert-Lachaine, H. Mecheri, C. Larue, A. Plamondon, Validation of inertial measurement units with an optoelectronic
343 system for whole-body motion analysis, *Med. Biol. Eng. Comput.* 55 (2017) 609–619. doi:10.1007/s11517-016-1537-2.
- 344 [11] D.T.P. Fong, Y.Y. Chan, The use of wearable inertial motion sensors in human lower limb biomechanics studies: A
345 systematic review, *Sensors (Switzerland).* 10 (2010) 11556–11565. doi:10.3390/s101211556.
- 346 [12] Z. Lin, M. Uemura, M. Zecca, S. Sessa, H. Ishii, M. Tomikawa, M. Hashizume, A. Takanishi, Objective skill evaluation
347 for laparoscopic training based on motion analysis, *IEEE Trans. Biomed. Eng.* 60 (2013) 977–985.
348 doi:10.1109/TBME.2012.2230260.
- 349 [13] D. Zhang, S. Sessa, W. Kong, S. Cosentino, D. Magistro, H. Ishii, M. Zecca, A. Takanishi, Development of subliminal
350 persuasion system to improve the upper limb posture in laparoscopic training: a preliminary study, *Int. J. Comput. Assist.*
351 *Radiol. Surg.* 10 (2015) 1863–1871. doi:10.1007/s11548-015-1198-x.
- 352 [14] S. Bolink, H. Naisas, R. Senden, H. Essers, I.C. Heyligers, K. Meijer, B. Grimm, Validity of an inertial measurement unit
353 to assess pelvic orientation angles during gait, sit-stand transfers and step-up transfers: Comparison with an optoelectronic
354 motion capture system, *Med. Eng. Phys.* 38 (2016) 225–231. doi:10.1016/j.medengphy.2015.11.009.
- 355 [15] A. Filippeschi, N. Schmitz, M. Miezal, G. Bleser, E. Ruffaldi, D. Stricker, Survey of Motion Tracking Methods Based on
356 Inertial Sensors: A Focus on Upper Limb Human Motion, *Sensors.* 17 (2017) 1257. doi:10.3390/s17061257.
- 357 [16] J.T. Zhang, A.C. Novak, B. Brouwer, Q. Li, Concurrent validation of Xsens MVN measurement of lower limb joint
358 angular kinematics, *Physiol. Meas.* 34 (2013). doi:10.1088/0967-3334/34/8/N63.
- 359 [17] G. Cooper, I. Sheret, L. McMillian, K. Siliverdis, N. Sha, D. Hodgins, L. Kenney, D. Howard, Inertial sensor-based knee
360 flexion/extension angle estimation, *J. Biomech.* 42 (2009) 2678–2685. doi:10.1016/j.jbiomech.2009.08.004.
- 361 [18] M. Al-Amri, K. Nicholas, K. Button, V. Sparkes, L. Sheeran, J. Davies, Inertial Measurement Units for Clinical

- 362 Movement Analysis: Reliability and Concurrent Validity, *Sensors*. 18 (2018) 719. doi:10.3390/s18030719.
- 363 [19] NOITOM, Axis Neuron Userguide, (2015) 1–127. <https://shopcdn.noitom.com.cn/software/AxisUserGuideFinal0923.pdf>.
- 364 [20] L. Zhang, M.M. Diraneyya, J.H. Ryu, C.T. Haas, E.M. Abdel-Rahman, Jerk as an indicator of physical exertion and
365 fatigue, *Autom. Constr.* 104 (2019) 120–128. doi:10.1016/j.autcon.2019.04.016.
- 366 [21] H. Kim, N. Hong, M. Kim, S. Yoon, H. Yu, H.-J. Kong, S.-J. Kim, Y. Chai, H. Choi, J. Choi, K. Lee, S. Kim, H. Kim,
367 Application of a Perception Neuron® System in Simulation-Based Surgical Training, *J. Clin. Med.* 8 (2019) 124.
368 doi:10.3390/jcm8010124.
- 369 [22] T. Dalager, K. Sogaard, K.T. Bech, O. Mogensen, P.T. Jensen, Musculoskeletal pain among surgeons performing
370 minimally invasive surgery: a systematic review, *Surg. Endosc.* 31 (2017) 516–526. doi:10.1007/s00464-016-5020-9.
- 371 [23] G. Lee, T. Lee, D. Dexter, R. Klein, A. Park, Methodological infrastructure in surgical ergonomics: A review of tasks,
372 models, and measurement systems, *Surg. Innov.* 14 (2007) 153–167. doi:10.1177/1553350607307956.
- 373 [24] S. Epstein, E. Sparer, B. Tran, Q. Ruan, J. Dennerlein, D. Singhal, B. Lee, Prevalence of Work-Related Musculoskeletal
374 Disorders among Surgeons and Interventionalists: A Systematic Review and Meta-analysis, *JAMA Surg.* 153 (2017) 1–
375 11.
- 376 [25] VICON, Vicon Motion Systems, (2018). <https://www.vicon.com/> (accessed January 5, 2018).
- 377 [26] L. Taylor, E. Miller, K.R. Kaufman, Static and dynamic validation of inertial measurement units, *Gait Posture.* 57 (2017)
378 80–84. doi:10.1016/j.gaitpost.2017.05.026.
- 379 [27] J. Craig, *Introduction to Robotics Mechanics and Control*, Pearson, 2004.
- 380 [28] J. Baek, H. Jeon, G. Kim, S. Han, Visualizing Quaternion Multiplication, *IEEE Access.* 5 (2017) 8948–8955.
381 doi:10.1109/ACCESS.2017.2705196.
- 382 [29] E. Bergamini, P. Guillon, V. Camomilla, H. Pillet, W. Skalli, A. Cappozzo, Trunk inclination estimate during the sprint
383 start using an inertial measurement unit: A validation study, *J. Appl. Biomech.* 29 (2013) 622–627.
384 doi:10.1123/jab.29.5.622.
- 385 [30] S. Kim, M.A. Nussbaum, Performance evaluation of a wearable inertial motion capture system for capturing physical
386 exposures during manual material handling tasks, *Ergonomics.* 56 (2013) 314–326. doi:10.1080/00140139.2012.742932.
- 387 [31] J. Bland, D. Altman, Statistical methods for assessing agreement between two methods of clinical measurement, *Lancet.*
388 (1986) 307–310. doi:10.1016/S0140-6736(86)90837-8.
- 389 [32] T. Kyun Kim, T Test as a Parametric Statistic, *Korean J. Anesthesiol.* 68 (2015) 540–546.
390 doi:10.4097/kjae.2015.68.6.540.
- 391 [33] T. Chai, R.R. Draxler, Root mean square error (RMSE) or mean absolute error (MAE)? -Arguments against avoiding
392 RMSE in the literature, *Geosci. Model Dev.* 7 (2014) 1247–1250. doi:10.5194/gmd-7-1247-2014.
- 393 [34] A. Ferrari, A.G. Cutti, A. Cappello, A new formulation of the coefficient of multiple correlation to assess the similarity of
394 waveforms measured synchronously by different motion analysis protocols, *Gait Posture.* 31 (2010) 540–542.

- 395 doi:10.1016/j.gaitpost.2010.02.009.
- 396 [35] T. Seel, J. Raisch, T. Schauer, IMU-Based Joint Angle Measurement for Gait Analysis, *Sensors*. 14 (2014) 6891–6909.
397 doi:10.3390/s140406891.
- 398 [36] R. Perez, U. Costa, M. Torrent, J. Solana, E. Opiisso, C. Ceceres, J.M. Tormos, J. Medina, E.J. Gemez, Upper limb
399 portable motion analysis system based on inertial technology for neurorehabilitation purposes, *Sensors*. 10 (2010) 10733–
400 10751. doi:10.3390/s101210733.
- 401 [37] A. Leardini, A. Chiari, U. Della Croce, A. Cappozzo, Human movement analysis using stereophotogrammetry Part 3. Soft
402 tissue artifact assessment and compensation, *Gait Posture*. 21 (2005) 212–225. doi:10.1016/j.gaitpost.2004.05.002.
- 403 [38] U. Della Croce, A. Leardini, L. Chiari, A. Cappozzo, Human movement analysis using stereophotogrammetry Part 4:
404 Assessment of anatomical landmark misplacement and its effects on joint kinematics, *Gait Posture*. 21 (2005) 226–237.
405 doi:10.1016/j.gaitpost.2004.05.003.
- 406 [39] J.L. McGinley, R. Baker, R. Wolfe, M.E. Morris, The reliability of three-dimensional kinematic gait measurements: A
407 systematic review, *Gait Posture*. 29 (2009) 360–369. doi:10.1016/j.gaitpost.2008.09.003.
- 408 [40] A.I. Cuesta-Vargas, A. Galán-Mercant, J.M. Williams, The use of inertial sensors system for human motion analysis,
409 *Phys. Ther. Rev.* 15 (2010) 462–473. doi:10.1179/1743288X11Y.0000000006.
- 410 [41] R. Takeda, S. Tadano, A. Natorigawa, M. Todoh, S. Yoshinari, Gait posture estimation by wearable acceleration and gyro
411 sensor, *IFMBE Proc.* 25 (2009) 111–114. doi:10.1007/978-3-642-03889-1-30.
- 412 [42] E. Allseits, K.J. Kim, C. Bennett, R. Gailey, I. Gaunard, V. Agrawal, A novel method for estimating knee angle using
413 two leg-mounted gyroscopes for continuous monitoring with mobile health devices, *Sensors (Switzerland)*. 18 (2018).
414 doi:10.3390/s18092759.
- 415
- 416